JACS
JOURNAL OF THE AMERICAN CHEMICAL SOCIETY
Communication
Cite This: J. Am. Chem. Soc. 2017, 139, 18182−18185
pubs.acs.org/JACS

Visualizing Intercellular Tensile Forces by DNA-Based Membrane Molecular Probes

Bin Zhao,[†] Casey O'Brien,[†] Aruni P. K. K. Karunanayake Mudiyanselage,[†] Ningwei Li,[§] Yousef Bagheri,[†] Rigumula Wu,[†] Yubing Sun,[§] and Mingxu You*[,†]

[†]Department of Chemistry, University of Massachusetts, Amherst, Massachusetts 01003, United States
[§]Depart of Mechanical & Industrial Engineering, University of Massachusetts, Amherst, Massachusetts 01003, United States

Supporting Information

ABSTRACT: Mechanical forces play critical roles in collective cell behaviors such as cell migration, proliferation, and differentiation. Extensive efforts have been made to measure forces between cells and extracellular matrices. However, force studies at cell−cell junctions remain a challenge. Herein, we reported a novel strategy to construct membrane DNA tension probes to visualize tensile forces at cell junctions. These lipid-modified probes can self-assemble onto cell membranes with high efficiency and stability. Upon experiencing tensile forces generated by neighboring cells, unfolding of the probes leads to a large increase in the fluorescence intensity. Compatible with readily accessible fluorescence microscopes, these easy-to-use membrane DNA tension probes can be broadly used to measure intercellular tensile forces.

Mechanical forces generated or experienced by cells are critical regulators of cell adhesions, signaling, and functions.[1] Transmembrane adhesion proteins, such as integrins and cadherins, can mediate and transmit mechanical forces between the cell and its microenvironment.[2] This biomechanical microenvironment includes both extracellular matrices and neighboring cells. Several techniques have been developed to measure mechanical forces between cells and extracellular matrices,[1] including traction force microscopy,[3] as well as collagen gel,[4,5] tissue pillar,[6,7] micropillar,[8] and molecular force sensors.[9−11] These techniques have laid the foundation for our understanding of the influence of environmental forces on various cellular functions. In contrast, the mechanical interactions between individual cells are still largely uninvestigated, mainly due to difficulty in modifying and controlling functional probes at complex cell−cell interfaces.[1,12]

Currently, three strategies have been developed to study intercellular forces. The first method, termed monolayer stress microscopy, utilizes cell-matrix traction force data to deduce mechanical forces at cell−cell junctions, with the assumption that the total forces experienced by each cell remain zero.[13] However, this method can only be applied to a monolayer of cells, requires extensive image analysis and data processing and, therefore, is not broadly used by the biological community. Another method utilizes microfabricated cantilever beams to deduce tugging forces between a pair of cells on bowtie-shaped micropatterns based on traction force measurements.[14] This approach requires advanced microfabrication facilities and can only measure forces between a single pair of cells at one time. The third strategy leverages molecular tension probes based on distance-dependent fluorescence resonance energy transfer (FRET) between fluorescent protein pairs.[15] In this strategy, the fluorescent proteins are genetically incorporated into certain types of cell−cell junction proteins.[15,16] However, many proteins cannot tolerate insertion of a ∼500 amino-acid-long sequence. In addition, the labor-intensive design and validation of the FRET sensors limit their routine usage. The limited force measurement range and low sensitivity further hinder the widespread applications of this approach.[17] Therefore, there are ever-increasing demands to develop more reliable and convenient probes to study intercellular forces.

Herein we report a novel membrane DNA tension probe (MDTP) to visualize intercellular tensile forces. As shown in Figure 1, the MDTP is composed of three oligonucleotides assembled through hybridization of 21-mer DNA handles: a cholesterol-modified stem-loop DNA hairpin anchor strand (black), a ligand- and fluorophore (6-fluorescein)-conjugated

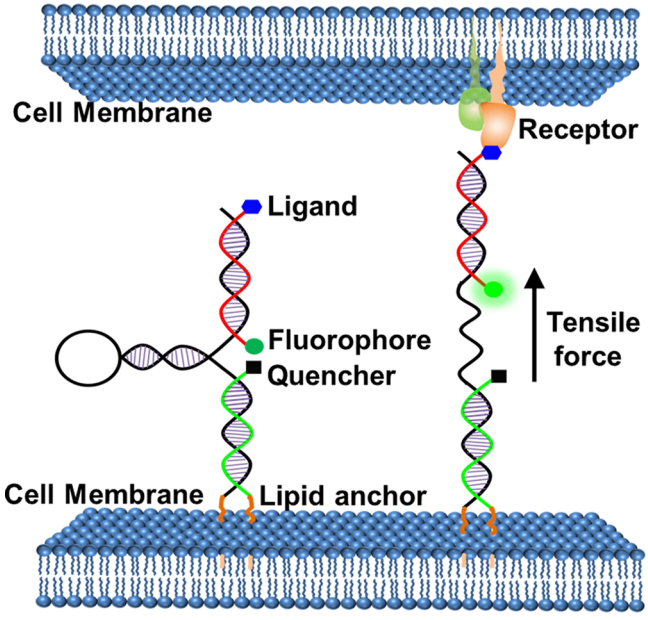

Figure 1. Schematic illustration of membrane DNA tension probe.

Received: October 19, 2017
Published: December 6, 2017

DOI: 10.1021/jacs.7b11176
J. Am. Chem. Soc. 2017, 139, 18182−18185

receptor-binding strand (red), and a cholesterol- and quencher (Epoch Eclipse)-labeled co-anchor strand (green). The self-assembled probe presents a pair of cholesterol anchors at one end, allowing the DNA probe to be spontaneously inserted onto a live cell membrane through hydrophobic interactions.[18−21] Once the tensile force exerted by a neighboring cell exceeds the threshold force to unfold the DNA hairpin, the fluorophore separates from the quencher, leading to an increase in fluorescence intensity. To validate our probe, we chose to study tensile forces induced by integrins and E-cadherins, two well-known transmembrane adhesion proteins that sense tensile forces and regulate cell functions accordingly.[2,22]

We first chemically conjugated a cyclic Arg-Gly-Asp-D-Phe-Lys (cRGDfk) ligand at the terminus of the tension probe, termed RGD-MDTP, to visualize integrin-mediated tensile forces. The RGD-modified DNA strand was prepared using a heterobifunctional cross-linker, sulfo-SMCC, and characterized with a gel mobility shift assay (Figure S1) and MALDI mass spectrometry (Table S1). A previously reported DNA hairpin strand containing 22% GC in the stem region was used to endow a tensile force tolerance of 4.2 pN.[10] The final RGD-MDTP structure was self-assembled by hybridization of three DNA strands. Agarose gel analysis confirmed the formation of the RGD-MDTP (Figure S2). The quenching efficiency (QE) in the absence of external forces was determined to be 79%. We obtained this number based on the fluorescence intensity ratio between the RGD-MDTP and the same probe without quencher modification, termed RGD-nqMDTP (Figure S2).

We next asked if the RGD-MDTP could be anchored onto the membranes of cell lines that are sensitive to cell mechanics, such as NIH/3T3 mouse embryonic fibroblast cells. Our result indicated that highly efficient probe insertion and long-term cell membrane persistence were observed with 3T3 cells in HEPES-containing saline buffer. The anchoring of RGD-nqMDTP onto cell membranes was clearly observed within 30 min of incubation (Figures 2a and S3a). Moreover, after removing excess probe in the solution, the inserted probe remained stable on the cell membranes for ∼4 h (Figure S3a). This efficient membrane anchoring was rooted in cholesterol-mediated hydrophobic interaction instead of RGD−integrin interactions (Figure S3b).

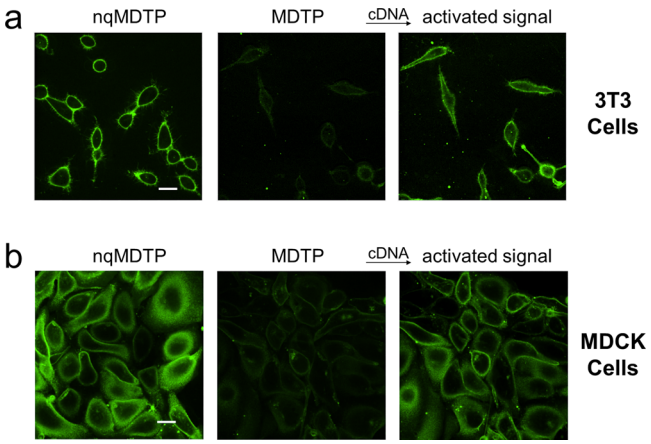

Figure 2. Highly efficient insertion and signal activation of MDTP on 3T3 (a) and MDCK (b) cell membrane. The addition of 5 μM of cDNA was used in this experiment. Scale bar: 20 μm.

We next asked if the function of the MDTP is still maintained on the cell membrane. With conjugated quencher, the MDTP (without RGD) induced a much lower membrane fluorescence signal than that of the nqMDTP, indicating the membrane folding of the MDTP. To further confirm the membrane unfolding event of MDTP, a complementary DNA strand (cDNA) was added after membrane anchoring of the MDTP. The cDNA can bind and open the hairpin region and separate the fluorophore from quencher, leading to recovery of the fluorescence signal. As expected, activated membrane signal was observed after adding cDNA (Figure 2a), suggesting the successful unfolding of the MDTP on the cell membranes.

We then utilized the MDTP to visualize integrin-induced tensile forces at cell−cell junctions. Here, integrin tensile forces generated by neighboring cells were directed to unfold the RGD-modified hairpin probe, RGD-MDTP, and an enhanced fluorescence signal was observed at cell−cell junctions (Figure 3a). Due to the intrinsic rigidity and negative charge nature of double-stranded DNA, the MDTP can "stand" on the negatively charged cell membrane, favoring the sensing of tensile forces between cells.

To confirm that the membrane fluorescence reflects integrin-induced tensile forces, but not other cellular events, we first

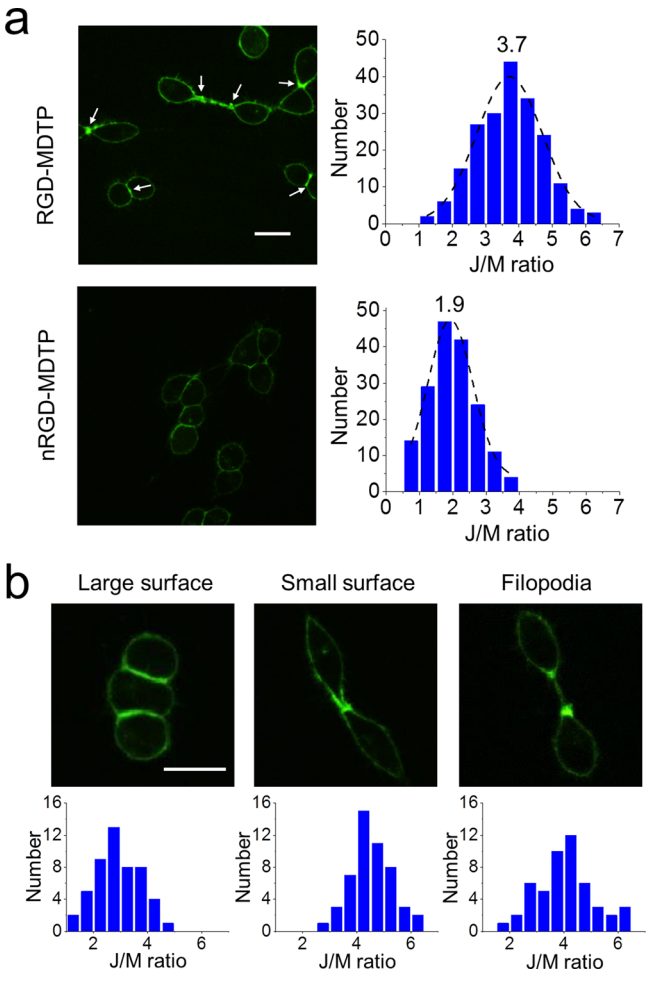

Figure 3. Visualizing integrin tension with MDTP. (a) Representative image showing activated fluorescence with RGD-MDTP (top left) and its distribution plot of junction/membrane fluorescence ratio (top right, 200 cell−cell contacts were measured). Results for nRGD-MDTP are shown as a control (bottom). (b) Representative images of different types of integrin-mediated adhesions as visualized with RGD-MDTP and their corresponding distribution plots. Scale bar: 20 μm.

DOI: 10.1021/jacs.7b11176
J. Am. Chem. Soc. 2017, 139, 18182−18185

quantitatively compared the results of the RGD-MDTP with the same DNA probe without attaching the adhesive peptide (nRGD-MDTP). Each individual intercellular fluorescence was binned according to its relative Junction brightness compared to the average Membrane fluorescence on the same cell, defined as J/M ratio (Figure S5). An average of 3.7-fold higher fluorescence was observed at the interface compared to other membrane regions with RGD-MDTP (Figure 3a). As a comparison, the J/M ratio of the nRGD-MDTP markedly reduced to 1.9, likely due to the increased local probe density from two neighboring cell membranes. The distinct difference of J/M ratio between RGD-MDTP and nRGD-MDTP indicates that RGD-MDTP can indeed be used to sense and visualize integrin-induced tensions between cells. As another control, such fluorescence signal is not due to the RGD-induced intercellular clustering formation (Figure S6).

Interestingly, we found that the integrin tensile force obviously varied among three different classes of 3T3 intercellular boundaries, namely large surface, small surface, and filopodia adhesions (Figure 3b).[23] Distribution plots of the J/M ratio revealed that both large surface and small surface adhesions have largely symmetric distributions, while filopodia adhesions showed a more heterogeneous distribution. Most small surface and filopodia adhesions displayed higher J/M ratio than that of large surface adhesions, implying that larger molecular tensile forces may be needed to maintain these two classes of adhesions in small contact areas. This result suggested that, the MDTP can be potentially used to study the heterogeneity of collective cell behaviors.

We further applied the MDTP to visualize E-cadherin-induced intercellular tensile forces. An E-cadherin on one cell membrane can bind with another E-cadherin on a neighboring cell in a homophilic binding manner.[24] E-cadherin-modified DNA tension probe (E-cad-MDTP) was prepared using a Protein G bridge to couple IgG/Fc-fused E-cadherin and DNA probe, in order to avoid activity loss resulted from direct chemical conjugation (Figure S7).[25] Protein G-DNA conjugate (ProG-LS) was first synthesized with a sulfo-SMCC linker and then self-assembled with quencher-labeled co-anchor strand and 22% GC hairpin anchor strand to prepare the ProG-MDTP. Finally, the E-cad-MDTP was obtained through the binding of the ProG-MDTP with IgG/Fc-fused E-cadherin. Gel mobility shift assays were used to confirm the probe formation (Figure S8a–d). The QE of the pre-assembled E-cad-MDTP was estimated to be 60% (Figure S8e).

After confirming the high expression level of membrane E-cadherin on a model epithelial cell line, MDCK (Figure S9), we then studied the anchoring efficiency of the pre-assembled E-cad-MDTP on these cell membranes. Unexpectedly, a large number of bright fluorescent spots appeared during the probe incubation with cells (Figure S10). Previous reports suggested that highly hydrophobic DNA-lipid conjugates may aggregate in the form of stable micelles,[26] which may not completely disassemble when encountering cell membranes.[18,20] Instead, the stepwise addition of DNA strands may prevent the aggregation and minimize the spots generated on the cell membranes. Indeed, a homogeneous membrane fluorescence signal was observed when employing stepwise addition (Figures S10 and 2b). In addition, *in situ* stepwise-assembled probe exhibited an improved QE (~80%) on the cell membranes. A rapid increase in membrane fluorescence intensity was observed after adding cDNA, indicating the successful unfolding of the ProG-MDTP (Figure 2b). These results together indicated that the stepwise-assembled E-cad-MDTP can be efficiently anchored onto the cell membrane and maintain the structure and function of the probe.

We next applied the stepwise-assembled E-cad-MDTP to visualize E-cadherin-induced intercellular tensile forces. An activated fluorescence signal was observed at the MDCK cell–cell interface. As a control, cells treated with the ProG-MDTP displayed much lower interfacial signals (Figures 4a and S11). To

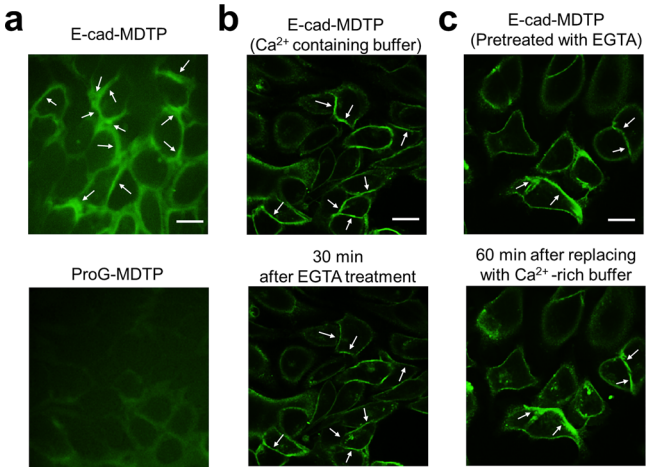

Figure 4. Visualization of E-cadherin-mediated tension at cell–cell junctions. (a) Representative images of MDCK cells anchored with E-cad-MDTP and ProG-MDTP. (b) Disruption of E-cadherin-induced tension by post-treating E-cad-MDTP-inserted cells with 10 mM EGTA. (c) Reconstitution of E-cadherin-mediated tension by addition of excess Ca^{2+}. Scale bar: 20 μm.

further confirm that the unfolding of probe was indeed induced by E-cadherin-mediated interactions, we added a Ca^{2+} chelating agent, EGTA. Calcium ions can increase the rigidity of the E-cadherin extracellular domains and are required for intercellular E-cadherin interactions. The addition of EGTA results in the substantial loss of free Ca^{2+}, which disrupts the E-cadherin-mediated adhesions.[27] Indeed, upon chelation of calcium ions, decreased fluorescence intensity was observed at cell–cell contacts due to the refolding of the DNA hairpin in the E-cad-MDTP.[28] Meanwhile, cells appeared to dissociate from each other because of the disruption of E-cadherin-mediated adhesions (Figure 4b). In another experiment, we pretreated the MDCK cells with EGTA and observed elevated force signals after replacing the Ca^{2+}-free buffer with a Ca^{2+}-rich solution. Indeed, reconstitution of E-cadherin-mediated adhesion resulted in tension-induced unfolding of the E-cad-MDTP (Figure 4c). As a control, the ProG-MDTP did not show any change in the fluorescence signal during either EGTA treatment (Figure S12). Taken together, we demonstrated that MDTP could be used to visualize E-cadherin-mediated intercellular tensile forces.

The sequence, duplex length, and shape of DNA probes can be rationally tuned to adjust their force tolerance, ranging from 1 to 50 pN,[9,17,29] to study a broad range of intercellular forces. Based on a similar design principle, more studies can be easily undertaken to visualize and quantify various types of intercellular forces. The membrane DNA tension probes are ideally suited for this application, for the following reasons: (1) in contrast to genetically encoded FRET sensors,[15] DNA probes function simply by incubation and self-assembly onto the cell membrane, avoiding the need for more difficult and time-consuming cloning or transfection; (2) DNA can be easily modified with various fluorophores and chemical moieties, potentially allowing

DOI: 10.1021/jacs.7b11176
J. Am. Chem. Soc. 2017, 139, 18182–18185

simultaneous study of different types of intercellular forces based on multicolor imaging; (3) broad choices of organic fluorophores can provide much higher signal-to-noise ratios compared to low-efficiency fluorescent protein-based FRET pairs,[30] thus making these DNA probes potentially useful in single-molecule force measurements in cells; and (4) in principle, these DNA probes can be used to quantify three-dimensional intercellular forces in physiologically relevant multilayer cellular assemblies, tissues, or entire organisms. Indeed, in this study, 3D imaging of integrin-induced tensile forces has been achieved (Figure S4). Of note, this strategy may be currently limited by the anchoring persistence of the DNA probes on cell membranes (~4 h). We are exploring the membrane-anchoring efficiency of other lipid modifications for long-term study of intercellular forces.

In conclusion, based on the rational design of lipid-anchored DNA probes, we have developed an innovative and universal membrane DNA tension probe to visualize intercellular tensile forces. Highly efficient probe insertion and signal activation on cell membranes have been demonstrated. By altering the ligand modification, cellular tensile forces mediated by either integrin or E-cadherin can be revealed. To the best of our knowledge, this is the first attempt to study intercellular forces using DNA-based molecular probes. We will further use the MDTP to study intercellular forces in various collective cell processes, including cancer cell invasion, wound healing, and embryo development.[31−34] These probes will be also potentially useful for developing novel strategies for tissue engineering and regenerative medicine.

■ ASSOCIATED CONTENT

Supporting Information

The Supporting Information is available free of charge on the ACS Publications website at DOI: 10.1021/jacs.7b11176.

Figures S1−S12, Table S1, and description of materials and methods (PDF)

■ AUTHOR INFORMATION

Corresponding Author

*mingxuyou@chem.umass.edu

ORCID

Mingxu You: 0000-0002-5279-2340

Notes

The authors declare no competing financial interest.

■ ACKNOWLEDGMENTS

The authors gratefully acknowledge the start-up grant from UMass, NSF CMMI 1662835 to Y.S., and IALS M2M seed grant. We are grateful to Dr. James Chambers for the assistance in fluorescence imaging, and Dr. Kathryn R. Williams and Ms. Tianxi Yang for help with manuscript preparation. We also thank every other member of the lab and Dr. Craig Martin for useful discussions. We also acknowledge the Light Microscopy Facility (UMass Amherst) where microscopy data were gathered.

■ REFERENCES

(1) Polacheck, W. J.; Chen, C. S. *Nat. Methods* **2016**, *13*, 415−423.
(2) Chen, C. S.; Tan, J.; Tien, J. *Annu. Rev. Biomed. Eng.* **2004**, *6*, 275−302.
(3) Legant, W. R.; Choi, C. K.; Miller, J. S.; Shao, L.; Gao, L.; Betzig, E.; Chen, C. S. *Proc. Natl. Acad. Sci. U. S. A.* **2013**, *110*, 881−886.
(4) Bell, E.; Ivarsson, B.; Merrill, C. *Proc. Natl. Acad. Sci. U. S. A.* **1979**, *76*, 1274−1278.
(5) Delvoye, P.; Wiliquet, P.; Levêque, J.-L.; Nusgens, B. V.; Lapière, C. M. *J. Invest. Dermatol.* **1991**, *97*, 898−902.
(6) Zimmermann, W. H.; Fink, C.; Kralisch, D.; Remmers, U.; Weil, J.; Eschenhagen, T. *Biotechnol. Bioeng.* **2000**, *68*, 106−114.
(7) Legant, W. R.; Pathak, A.; Yang, M. T.; Deshpande, V. S.; McMeeking, R. M.; Chen, C. S. *Proc. Natl. Acad. Sci. U. S. A.* **2009**, *106*, 10097−10102.
(8) Tan, J. L.; Tien, J.; Pirone, D. M.; Gray, D. S.; Bhadriraju, K.; Chen, C. S. *Proc. Natl. Acad. Sci. U. S. A.* **2003**, *100*, 1484−1489.
(9) Blakely, B. L.; Dumelin, C. E.; Trappmann, B.; McGregor, L. M.; Choi, C. K.; Anthony, P. C.; Duesterberg, V. K.; Baker, B. M.; Block, S. M.; Liu, D. R.; Chen, C. S. *Nat. Methods* **2014**, *11*, 1229−1232.
(10) Zhang, Y.; Ge, C.; Zhu, C.; Salaita, K. *Nat. Commun.* **2014**, *5*, 5167.
(11) Chang, Y.; Liu, Z.; Zhang, Y.; Galior, K.; Yang, J.; Salaita, K. *J. Am. Chem. Soc.* **2016**, *138*, 2901−2904.
(12) Eisenstein, M. *Nature* **2017**, *544*, 255−257.
(13) Tambe, D. T.; Corey Hardin, C.; Angelini, T. E.; Rajendran, K.; Park, C. Y.; Serra-Picamal, X.; Zhou, E. H.; Zaman, M. H.; Butler, J. P.; Weitz, D. A.; Fredberg, J. J.; Trepat, X. *Nat. Mater.* **2011**, *10*, 469−475.
(14) Liu, Z.; Tan, J. L.; Cohen, D. M.; Yang, M. T.; Sniadecki, N. J.; Ruiz, S. A.; Nelson, C. M.; Chen, C. S. *Proc. Natl. Acad. Sci. U. S. A.* **2010**, *107*, 9944−9.
(15) Borghi, N.; Sorokina, M.; Shcherbakova, O. G.; Weis, W. I.; Pruitt, B. L.; Nelson, W. J.; Dunn, A. R. *Proc. Natl. Acad. Sci. U. S. A.* **2012**, *109*, 12568−12573.
(16) Conway, D. E.; Breckenridge, M. T.; Hinde, E.; Gratton, E.; Chen, C. S.; Schwartz, M. A. *Curr. Biol.* **2013**, *23*, 1024−1030.
(17) Wang, X.; Ha, T. *Science* **2013**, *340*, 991−994.
(18) Pfeiffer, I.; Höök, F. *J. Am. Chem. Soc.* **2004**, *126*, 10224−10225.
(19) You, M. X.; Lyu, Y. F.; Han, D.; Qiu, L. P.; Liu, Q. L.; Chen, T.; Wu, C. S.; Peng, L.; Zhang, L. Q.; Bao, G.; Tan, W. H. *Nat. Nanotechnol.* **2017**, *12*, 453−459.
(20) Weber, R. J.; Liang, S. I.; Selden, N. S.; Desai, T. A.; Gartner, Z. J. *Biomacromolecules* **2014**, *15*, 4621−4626.
(21) Liu, H.; Kwong, B.; Irvine, D. J. *Angew. Chem., Int. Ed.* **2011**, *50*, 7052−7055.
(22) Niessen, C. M.; Leckband, D.; Yap, A. S. *Physiol. Rev.* **2011**, *91*, 691−731.
(23) Bray, S. J. *Nat. Rev. Mol. Cell Biol.* **2016**, *17*, 722−735.
(24) Leckband, D. E.; de Rooij, J. *Annu. Rev. Cell Dev. Biol.* **2014**, *30*, 291−315.
(25) Wang, X.; Rahil, Z.; Li, I. T.; Chowdhury, F.; Leckband, D. E.; Chemla, Y. R.; Ha, T. *Sci. Rep.* **2016**, *6*, 21584.
(26) Liu, H.; Zhu, Z.; Kang, H.; Wu, Y.; Sefan, K.; Tan, W. *Chem. - Eur. J.* **2010**, *16*, 3791−3797.
(27) Rothen-Rutishauser, B.; Riesen, F. K.; Braun, A.; Günthert, M.; Wunderli-Allenspach, H. *J. Membr. Biol.* **2002**, *188*, 151−162.
(28) Liphardt, J.; Onoa, B.; Smith, S. B.; Tinoco, I.; Bustamante, C. *Science* **2001**, *292*, 733−737.
(29) Iwaki, M.; Wickham, S. F.; Ikezaki, K.; Yanagida, T.; Shih, W. M. *Nat. Commun.* **2016**, *7*, 13715.
(30) Jurchenko, C.; Salaita, K. S. *Mol. Cell. Biol.* **2015**, *35*, 2570−2582.
(31) Wozniak, M. A.; Chen, C. S. *Nat. Rev. Mol. Cell Biol.* **2009**, *10*, 34−43.
(32) Bazellières, E.; Conte, V.; Elosegui-Artola, A.; Serra-Picamal, X.; Bintanel-Morcillo, M.; Roca-Cusachs, P.; Muñoz, J. J.; Sales-Pardo, M.; Guimerà, R.; Trepat, X. *Nat. Cell Biol.* **2015**, *17*, 409.
(33) Li, L.; He, Y.; Zhao, M.; Jiang, J. *Burns Trauma* **2013**, *1*, 21−26.
(34) Friedl, P.; Gilmour, D. *Nat. Rev. Mol. Cell Biol.* **2009**, *10*, 445−457.

DOI: 10.1021/jacs.7b11176
J. Am. Chem. Soc. 2017, 139, 18182−18185